Biochimica et Biophysica Acta 1840 (2014) 2171–2183

Contents lists available at ScienceDirect

Biochimica et Biophysica Acta

journal homepage: www.elsevier.com/locate/bbagen

p19INK4d is involved in the cellular senescence mechanism contributing to heterochromatin formation

Silvina V. Sonzogni, María Florencia Ogara, Laura M. Belluscio, Daniela S. Castillo, María E. Scassa, Eduardo T. Cánepa *

Laboratorio de Biología Molecular, Departamento de Química Biológica, Facultad de Ciencias Exactas y Naturales, Universidad de Buenos Aires, Ciudad Universitaria, Pabellón II, 1428 Ciudad de Buenos Aires, Argentina

ARTICLE INFO

Article history:
Received 23 October 2013
Received in revised form 26 February 2014
Accepted 11 March 2014
Available online 22 March 2014

Keywords:
Cellular senescence
CDK inhibitor
DNA damage
Heterochromatin
Aging

ABSTRACT

Background: During evolution, organisms with renewable tissues have developed mechanisms to prevent tumorigenesis, including cellular senescence and apoptosis. Cellular senescence is characterized by a permanent cell cycle arrest triggered by both endogenous stress and exogenous stress. The p19INK4d, a member of the family of cyclin-dependent kinase inhibitors (INK4), plays an important role on cell cycle regulation and in the cellular DNA damage response. We hypothesize that p19INK4d is a potential factor involved in the onset and/or maintenance of the senescent state.
Methods: Senescence was confirmed by measuring the cell cycle arrest and the senescence-associated β-galactosidase activity. Changes in p19INK4d expression and localization during senescence were determined by Western blot and immunofluorescence assays. Chromatin condensation was measured by micrococcal nuclease digestion and histone salt extraction.
Results: The data presented here show for the first time that p19INK4d expression is up-regulated by different types of senescence. Changes in senescence-associated hallmarks were driven by modulation of p19 expression indicating a direct link between p19INK4d induction and the establishment of cellular senescence. Following a senescence stimulus, p19INK4d translocates to the nucleus and tightly associates with chromatin. Moreover, reduced levels of p19INK4d impair senescence-related global genomic heterochromatinization. Analysis of p19INK4d mRNA and protein levels in tissues from differently aged mice revealed an up-regulation of p19INK4d that correlates with age.
Conclusion: We propose that p19INK4d participates in the cellular mechanisms that trigger senescence by contributing to chromatin compaction.
General significance: This study provides novel insights into the dynamics process of cellular senescence, a central tumor suppressive mechanism.

1. Introduction

Cellular senescence refers to the essentially irreversible growth arrest induced at the end of the cellular lifespan or in response to different types of stress [1–3]. With the possible exception of embryonic stem cells, most cells undergo senescence when appropriately stimulated [4]. Senescence-inducing stimuli are multiple and each one precipitates a different type of senescence [5]. These findings have led to the distinction between "physiological or replicative senescence" triggered by a cell-intrinsic mechanism like eroded telomeres and "premature senescence" triggered by extrinsic stress like DNA damaging agents, oxidative stress or oncogene activation [1].

Physiological or replicative senescence depends on the activation of ataxia telangiectasia mutated (ATM) and checkpoint kinase 2 (Chk2) [6,7]. Genotoxic senescence, induced by agents that cause DNA damage, also depends on ATM and Chk2 [8,9]. By contrast, oncogene-induced senescence, the form that is most likely to be associated with human precancerous lesions, has been linked to increased expression of the tumor suppressors p16INK4a and ARF [10]. In addition, the two paradigmatic tumor suppressor proteins p53 and retinoblastoma (Rb) are activated

Abbreviations: Rb, retinoblastoma; SAHF, senescence associated heterochromatin foci; HP1, heterochromatin protein 1; SA-β-Gal activity, senescence associated beta galactosidase activity; DDR, DNA damage response; CPT, camptothecin; MEFs, mouse embryonic fibroblasts; MNase, micrococcal nuclease; CKI, CDK inhibitor

* Corresponding author at: Departamento de Química Biológica, Facultad de Ciencias Exactas y Naturales, Ciudad Universitaria, Pabellón II, Piso 4, 1428 Ciudad de Buenos Aires, Argentina. Tel./fax: +54 11 45763342.
E-mail address: ecanepa@qb.fcen.uba.ar (E.T. Cánepa).

http://dx.doi.org/10.1016/j.bbagen.2014.03.015
0304-4165/

upon entry into senescence. p53 is stabilized and proceeds to activate its main transcriptional target, p21CIP1/WAF1 [11]. Rb is found in its active, hypophosphorylated form, in which it binds to the E2F protein family members to repress their transcriptional targets which are required for cell-cycle progression [12].

A distinguishing aspect of cellular senescence is the development of global genome heterochromatinization [13]. Senescent cells display an overall increase in non-pericentromeric, facultative heterochromatin domains, known as senescence-associated heterochromatin foci (SAHF) [14,15]. SAHF is composed of repressive chromatin structures that prevent transcription of growth-promoting genes, particularly those targeted by the E2F family of transcription factors [16]. This evidence tempted us to speculate that SAHF would be involved in senescence mechanism through the inhibition of cell proliferation. Nevertheless, while the repression of cell cycle controllers is a central function of SAHF, the frequency and distribution of these foci, suggest a much wider role of SAHF [17]. SAHF contain several common markers of heterochromatin, including histones that are hypoacetylated, methylation of lysine 9 of histone H3 and bound heterochromatin protein 1 (HP1). SAHF are also characterized by their depletion of linker histone H1 and enrichment in at least two other proteins, namely histone variant macroH2A and HMGA [18,19].

An alternative point of view about the function of SAHF has been recently postulated [20]. According to this point of view, SAHF is formed as a result of persistent DNA damage. This hypothesis postulates the existence of two types of heterochromatin in senescent cells: one that represses cell cycle-regulating genes and the other that suppresses the DNA damage response (DDR). Formation of SAHF has been reported to depend on senescence effectors, like pRB and p53 [21]. Furthermore, senescent cells exhibit high levels of chromatin-bound HMGA proteins, indicating that these proteins are essential for SAHF formation [22]. Therefore, although the vast majority of the proteins involved in the senescence response network are known, many gaps remain to be filled in the integrated response organized by the cell.

p19INK4d is a member of the INK4 family of CDK inhibitors that includes p16INK4a, p15INK4b and p18INK4c. All members share structural features and, more importantly, the ability to bind to and inhibit cyclin/CDK complexes containing CDK4 or CDK6, contributing to cell cycle arrest at the G1 phase in response to multiple stress stimuli [23,24]. The INK4 family members are differentially expressed during mouse development and seem to be involved in the regulation of different cell cycle events like differentiation and senescence. Apart from their physiological roles, INK4 proteins are commonly lost or inactivated by mutations in diverse types of cancers, and represent established or candidate tumor suppressors [25,26]. In the last years, a novel and unique function of p19INK4d (hereafter referred to as p19) that distinguishes it from its siblings has been described. p19 has been shown to improve DNA repair and negatively modulate DNA damage-induced apoptosis in mammalian cells [27–29]. These properties, besides its well-known activity on cell cycle regulation, prompted us to hypothesize that p19 would belong to a protein network that would integrate DDR in order to maintain genomic integrity. Hence, and based on the above evidence, we asked whether p19 could be involved in the establishment of senescence.

In the present study we demonstrated that, in response to genotoxic or premature senescence stimuli, p19 is transcriptionally up-regulated. Once induced, p19 displays nucleus translocation and strongly binds to the chromatin. In the presence of senescent stimuli p19-deficient cells show delayed cell cycle arrest and decreased senescence-associated beta-galactosidase (SA-β-Gal) activity, both features closely associated with senescence [30]. Moreover, reduced levels of p19 impair senescence-related global genomic heterochromatinization. Finally, increased levels of p19 were observed in tissues of aged mice, suggesting a physiological relevance of the cellular mechanisms described here. We propose that p19 participates in the cellular mechanisms that trigger senescence by contributing to chromatin compaction.

2. Materials and methods

2.1. Senescence approach and cell cultures

For genotoxic senescence, we used camptothecin (CPT) which inhibits topoisomerase I causing double-stranded breaks. It has been reported that at low concentrations (20 nM) this drug induces senescence [31–33]. Mouse embryonic fibroblasts (MEFs) undergo premature senescence in culture after 5–10 passages, despite their retaining long telomeres. The senescence of MEFs has been recently shown to be a result of oxidative stress in culture [34,35]. MEFs were prepared from 14.5-day-old embryos from CF-1 mice as previously reported [36]. WI-38 (ATCC-CCL-75), non-SV40-transformed HEK293 (ATCC-CRL-1573) and BHK-21 (ATCC-CCL-10) cell lines were grown in DMEM (Invitrogen) supplemented with 10% fetal bovine serum (FBS), 100 U/ml penicillin, 100 mg/ml streptomycin, and 2 mM glutamine at 37 °C in a 5% CO_2 humidified atmosphere.

Stable cell lines, BHK-21p19S and BHK-21p19AS, were performed as previously described [37]. For metallothionein promoter induction cells were treated with 75 μM $ZnSO_4$ for at least 5 h.

2.2. RNA extraction and Northern blot analysis

RNA extraction and Northern blot analysis were carried out as previously described [38]. Briefly, total RNA was denatured, electrophoresed in 1% glyoxal-agarose gels, and transferred to nylon membranes (Hybond N, Amersham). Membranes were sequentially hybridized with the indicated [^{32}P]-labeled probes and radioactivity was detected using a PhosphorImager (FujiFilm BAS-1800II) and quantified using ImageJ software.

2.3. Nuclear run-on transcription assay

Nuclear run-on assays were performed as previously described [38]. Nuclear RNA was radiolabeled, extracted and hybridized to nylon membranes (GeneScreen Plus, PerkinElmer) previously slot-blotted with 10 pmol of specific single stranded DNA probes. Radioactivity was detected using a PhosphorImager (FujiFilm BAS-1800II) and quantified using ImageJ software.

2.4. Total cell extracts, nuclear extracts, and chromatin isolation

To prepare total cell extracts, cultured cells were harvested by centrifugation, washed in PBS, and directly resuspended in Laemmli buffer, followed by sonication for 15 s at 25% amplitude. Proteins were resolved in 15% polyacrylamide gels and analyzed by immunoblotting using monoclonal anti-human anti-p19 (P0999-55A, US Biological), or anti mouse anti-p19 (37-8700, Invitrogen), anti-γHP1 (MAB3450, Chemicom International), anti-β-actin (sc-477778, Santa Cruz) and anti-GAPDH (sc-32233, Santa Cruz) antibodies.

Chromatin was isolated as previously described [39]. To verify the correct separation of each fraction anti-GAPDH was used as a cytoplasm marker and anti-total histone H3 (sc-8654-R, Santa Cruz) as a chromatin marker.

2.5. Heterochromatin and euchromatin fractionation

Sub-nuclear fractions were obtained according to Frenster et al. [40]. Total cell extract, heterochromatin and euchromatin were directly resuspended in the same volume of Laemmli buffer 1× before proceeding to Western blot analysis. The correct separation was verified using anti-α-HP1 (AB-14298, ABCAM) as a heterochromatin marker and RNAPolII CTD4H8 (05-623, Millipore) as a euchromatin marker.

2.6. Histone salt extraction analyses and micrococcal nuclease digestion

Salt extraction analyses were performed as described previously [41]. Extracted histones were subjected to SDS-PAGE and analyzed by Western blot.

Nuclease digestion was performed as previously described [42]. Briefly, cells were resuspended in 1 ml of lysis buffer (10 mM Tris/HCl pH 7.5, 10 mM $MgCl_2$, 1 mM DTT, 0.5% NP-40) and incubated on ice for 5 min. Nuclear pellet was obtained by centrifugation and resuspended in digestion buffer (15 mM Tris–HCl pH 7.4, 60 mM KCl, 5 mM NaCl, 0.25 M sucrose, 1 mM $CaCl_2$, 0.5 mM DTT). Reaction volumes of 100 μl were pre-incubated at 32 °C with 0.2 U/μl MNase. DNA was purified by standard procedures and electrophoresis was carried out in 1% agarose gels.

2.7. Immuno-fluorescence and microscopy

Immunofluorescence and pre-extraction experiments with Triton X-100 were previously described [27,43]. For labeling p19 and γ-HP1, cells were incubated with polyclonal anti-rabbit anti-p19 (sc-1063, Santa Cruz) and mouse monoclonal anti-γHP1 (Chemicon International) diluted in 2% BSA. Cells were then washed three times for 10 min in PBS-0.1% Triton and incubated with Alexa Fluor 594 and Alexa Fluor 488 (Molecular Probes) for 1 h at 37 °C. Nuclear DNA was counterstained with 4,6 diamidino-2-phenylindole (DAPI, 2 μg/μl). Coverslips were mounted in Mowiol 4-88 antifading agent (Calbiochem). Image acquisition was performed with Olympus FluoView scanning laser biological inverted microscope IX70 using Zeiss AxioCam camera and quantified with cell image analysis software cell profiler.

2.8. Reporter assay

A site-directed mutagenesis of p19CATE2Fmut was performed as previously described [44]. The deletion-mutant plasmids p19CAT Δ1500, p19CATΔ1000, p19CATΔ750, p19CATΔ500, and p19CATΔ250 were generated by digestion of p19CATFL. Site directed mutagenesis and deletion-mutant plasmid were performed by Mutagenex, Inc.

HEK293 and BHK-21 cells were used for their high efficiency of transfection using the polyethyleneimine PEI (Polysciences, Inc.) method [45]. Briefly, cells seeded in six-well dishes were transfected with 4 μg CAT reporter plasmid and 4 μg of CMV-β-galactosidase. Total DNA amount was adjusted to 10 μg/well with non-specific DNA carrier. After 16 h of incubation, the culture medium was changed and treatments were carried out. Cells were harvested for CAT and β-galactosidase activity determination as previously described [46]. CAT activity was normalized to β-galactosidase activity. When indicated, cells were cotransfected with 2 μg of puroBABE and 8 μg of expression vector for mutant CDK4R24C (a generous gift of Patrick O' Connor, Bethesda). Twenty four hours after transfection, 2.5 μg/ml of puromycin (Sigma) was added for 48 h to select for transfected cells.

2.9. [^{3}H]Thymidine incorporation, cell proliferation and SA-β-gal assays

Thymidine incorporation was previously described [27]. For proliferation assay cells were plated in six-well dishes, fixed and stained with crystal violet. After extensive washing, crystal violet was resolubilized in 10% acetic acid and quantified at 595 nm as a relative measure of cell number.

SA-β-gal activity was detected as previously described [47]. Cells were examined at ×400 magnifications in inverted microscope IX70 using Zeiss AxioCam camera.

2.10. RNA and protein extraction from tissues in mice of different ages

Experiments were carried out in CF-1 male mice of different ages (1, 6, 12, 18 months). Mice were housed and treated in accordance with the Guide for Care and Use of Laboratory Animals, National Institutes of Health, published 80-23/96.

Mice were euthanized by cervical dislocation (n = 4 of each age). The liver, lung, kidney, pancreas, spleen, thymus, testicle, heart and brain were removed from each mouse. For RNA extraction ~100 mg of each organ was weighed and homogenized with 700 μl of denaturing solution and then processed for Northern blot analysis. For protein extraction, ~80 mg of each tissue was weighted and homogenized with 1000 μl of 2% SDS pH 6.8 and then incubated for 10 min at 70 °C and centrifuged at 14,000 rpm for 20 min. The supernatants were directly resuspended in Laemmli buffer 1× and sonicated for 15 s at 25% amplitude before proceeding to Western blot analysis.

3. Results

3.1. p19 is induced early in cellular senescence

To test whether p19 is induced in response to both genotoxic senescence and premature senescence, we first examined its transcript and protein levels by Northern blot and Western blot in various cell lines. Diploid embryonic human lung fibroblasts (WI-38) and SV40-negative human embryonic kidney (HEK293) and fibroblast from hamster kidney (BHK-21) were used for genotoxic senescence. MEFs and primary cultures of human skin cells were analyzed for premature and replicative senescence. WI-38 cells treated with CPT at different times displayed increased levels of both p19 mRNA and protein, reaching a maximum at 24 h after treatment, which was maintained for over 72 h (Fig. 1A and D). The induction was dose-dependent (Fig. 1B) and not limited to one cell type, since this phenomenon was observed in several cell lines (Supplementary Fig. S1C–F). Similarly, with regard to premature and replicative senescence, p19 was significantly induced in MEFs at P6 and at P4 in human fibroblasts and remained increased at later passages (Fig. 1C and F; Supplementary Fig. S1I).

Our models recapitulated properties of senescent cells since CPT-treated cells and MEFs, collected at later passages, showed increased size (Supplementary Fig. S2A and B), enlarged nuclei and DNA pattern of SAHF which was confirmed by the presence of γ-HP1, a known SAHF marker (Supplementary Fig. S2C and D). Moreover, 80% of CPT-treated WI-38 cells (Fig. 1H and I) and 46% of P6-MEFs (Fig. 1J and K) were positively stained for SA-β-gal activity.

In addition, the mRNA expression of senescence biomarkers p21 and p16 was strikingly increased, while that of p15, p18 and p27 remained unchanged (Fig. 1A–C; Supplementary Fig. S1A–C). Protein levels of p21 and p16 were consistently induced after CPT treatment (Fig. 1E; Supplementary Fig. S1G–H). Similarly, p21 and p16 were significantly increased in MEFs from P6 (Fig. 1G).

To verify the permanent senescence growth arrest, cell cycle progression was monitored by analysis of thymidine incorporation. The results showed that thymidine incorporation was barely detected in CPT-treated WI-38 and BHK-21 cells (Fig. 1L and Supplementary Fig. S2E). Likewise, thymidine incorporation in MEFs began to decrease at P5 and remained at minimum levels at later passages (Fig. 1M). In addition, cells treated with CPT for 24 h and then cultured in CPT-free medium for 8 days showed no proliferation, in contrast with untreated cells, which showed exponential growth (Supplementary Fig. S2F). Similarly, MEF proliferation began to decrease after P3 (Supplementary Fig. S2G).

Interestingly, the increase in p19 transcript was temporarily overlapped with p21 and p16 up-regulation. In addition, p19 increase occurred simultaneously with the onset of senescence-associated cell markers, suggesting that its induction arose early in response to the stimulus that triggers senescence.

3.2. p19 levels modulate the senescence program

Given that p19 expression is early induced in response to senescence, we wondered whether p19 protein plays a causal role in this

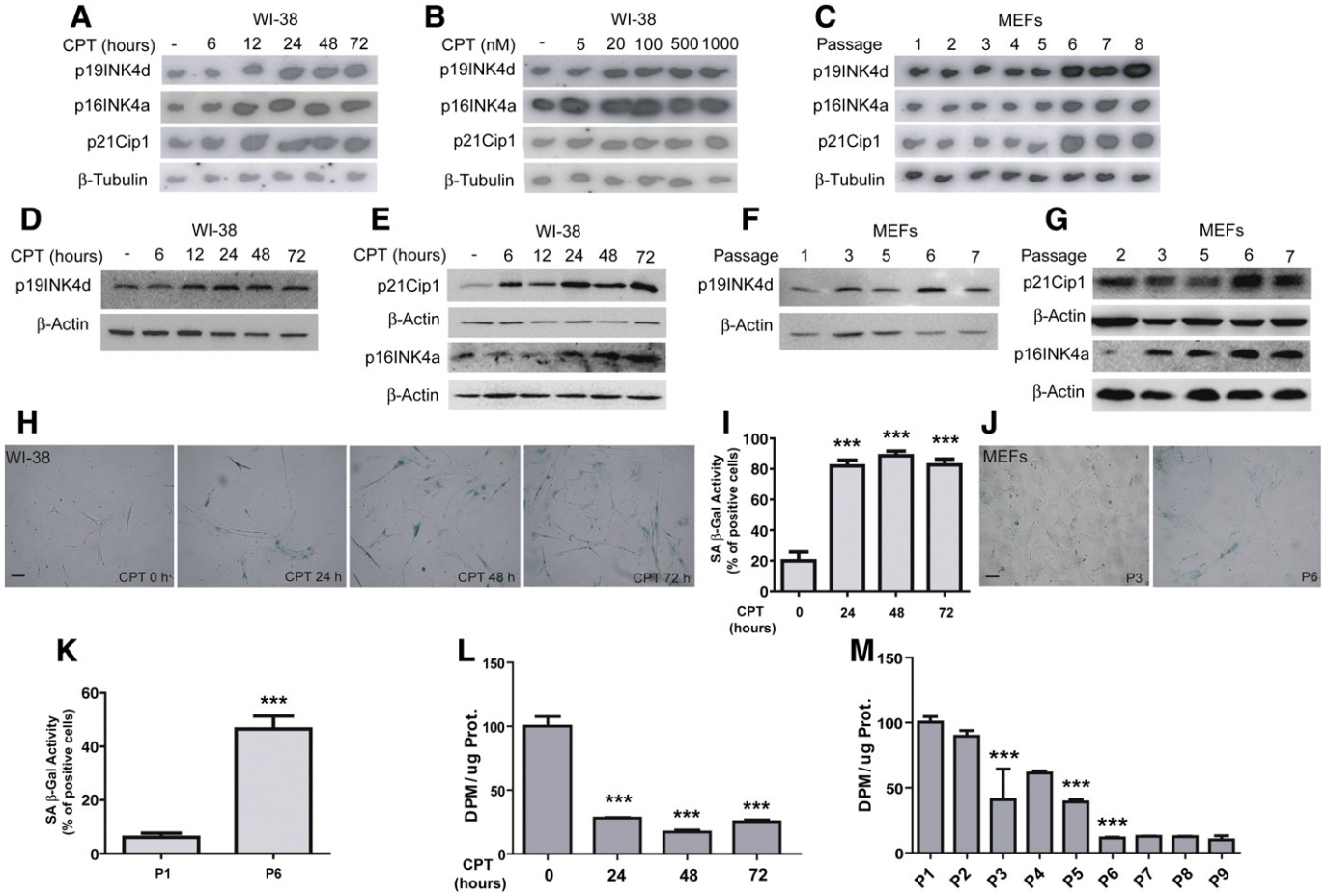

Fig. 1. p19 up-regulation and senescent-related biomarkers in both senescence models. (A, D and E) WI-38 cells were exposed to 20 nM CPT at various time points. (B) WI-38 cells were treated with different doses of CPT for 24 h. (C, F) MEFs were collected at different passages in culture. (A, B, C) Total RNA (20 μg) was subjected to Northern blot analysis with the ^{32}P-labeled probes indicated at the left margin. (D, E, F and G) Equal amount of protein from cell lysates prepared at indicated time or passages was subjected to 15% SDS-PAGE, transferred to nitrocellulose membrane and analyzed by Western blot with p19, p16, p21 and β-actin antibodies. Results showed in the figure are representative of at least three independent experiments. (H) WI-38 cells treated with 20 nM CPT for 24, 48 and 72 h and (J) MEFs at P3 and P6 were cytochemically analyzed for SA-β-Gal activity at pH 6.0 (scale bar 20 μm). (I, K) Percentages of SA-β-Gal positively stained cells were quantified and are presented as mean ± SEM of 6 fields analyzed for each sample. (I) $F_{3,19} = 55.68$, ***$p < 0.0001$ (one-way ANOVA followed by Bonferroni's post-test, 0 h vs. 24 h, ***$p < 0.001$; 0 h vs. 48 h, ***$p < 0.001$; 0 h vs. 72 h, ***$p < 0.001$). (K) ***$p < 0.0001$ Student's *t* test was performed to compare SA-β-Gal activity at P1 vs. P6 in MEFs. (L) WI-38 cells treated with CPT for different time periods and (M) MEFs collected at different passages in culture, were incubated with 1 μCi/ml [^{3}H]-thymidine for 6 h at 37 °C. Cells were lysed and thymidine incorporation was measured as DPM/μg protein. Results were statistically analyzed by one-way ANOVA followed by Bonferroni's post-test. (L) $F_{3,8} = 90.48$, ***$p < 0.0001$; 0 h vs. 24 h, ***$p < 0.001$; 0 h vs. 48 h, ***$p < 0.001$; 0 h vs. 72 h, ***$p < 0.001$. (M) $F_{8,27} = 17.74$, ***$p < 0.0001$; P1 vs. P3, ***$p < 0.001$; P1 vs. P5, ***$p < 0.001$; P1 vs. P6, ***$p < 0.001$.

mechanism. In order to challenge this hypothesis, BHK-21 cells stably transfected with p19 cDNA in a sense (BHK21-p19S) or antisense (BHK21-p19AS) orientation were treated with 20 nM CPT (Supplementary Fig. S3A and B). We observed a significant delay in thymidine incorporation in CPT-treated BHK21-p19AS compared to BHK21-p19S or BHK-21WT cells (Fig. 2A). Moreover, the number of CPT-treated cells that expressed SA-β-gal activity was greatly increased in BHK21-p19S cells as compared with SA-β-gal-expressing p19AS or WT cells (Fig. 2B and C). These results strongly suggest that there is a direct relationship between p19 induction and the establishment of senescence.

3.3. Up-regulation of p19 expression depends on the genotoxic doses used

We have previously reported that p19 is involved in DNA repair and cell survival [27,28,37]. Therefore, we wondered whether senescence-associated p19 induction would be linked to its up-regulation following a DNA damaging stimulus. To test this, WI-38 cells were exposed either to low (20 nM) or high (1 μM) CPT concentrations for 24 h, i.e., cells were treated with a senescent or a DNA damaging stimulus respectively as previously reported [32,33]. Afterwards, the cells were cultured in CPT-free medium for 4 days (Fig. 3A). The rationale was that a DNA damage response would involve a transient p19 induction, while a senescence stimulus would cause a persistent p19 up-regulation even if CPT was removed.

We observed that cells treated with low doses of CPT for 24 h displayed a significant p19 up-regulation that was maintained for at least 4 days. In contrast, cells treated with high CPT doses showed a higher but transient p19 induction (Fig. 3B).

In agreement with senescence-associated cell cycle arrest, cell cultures incubated with 20 nM CPT exhibited no significant changes in cell number (Fig. 3C). Conversely, cell cultures incubated with 1 μM CPT showed a decrease in cell number, probably caused by apoptosis, in agreement with previous reports [33].

3.4. p19 induction is regulated at the transcriptional level during senescence

The increased p19 mRNA levels in both premature senescence and genotoxic senescence could have different causes, including changes in the transcriptional rate levels. To study the effect of genotoxic senescence and premature senescence on the transcription initiation rate of p19, we performed a run-on assay. p19 transcription showed a 3-fold increase in CPT-treated cells compared to untreated cells. Similarly, the transcriptional rate level of p19 was 2-fold higher in MEFs at P6

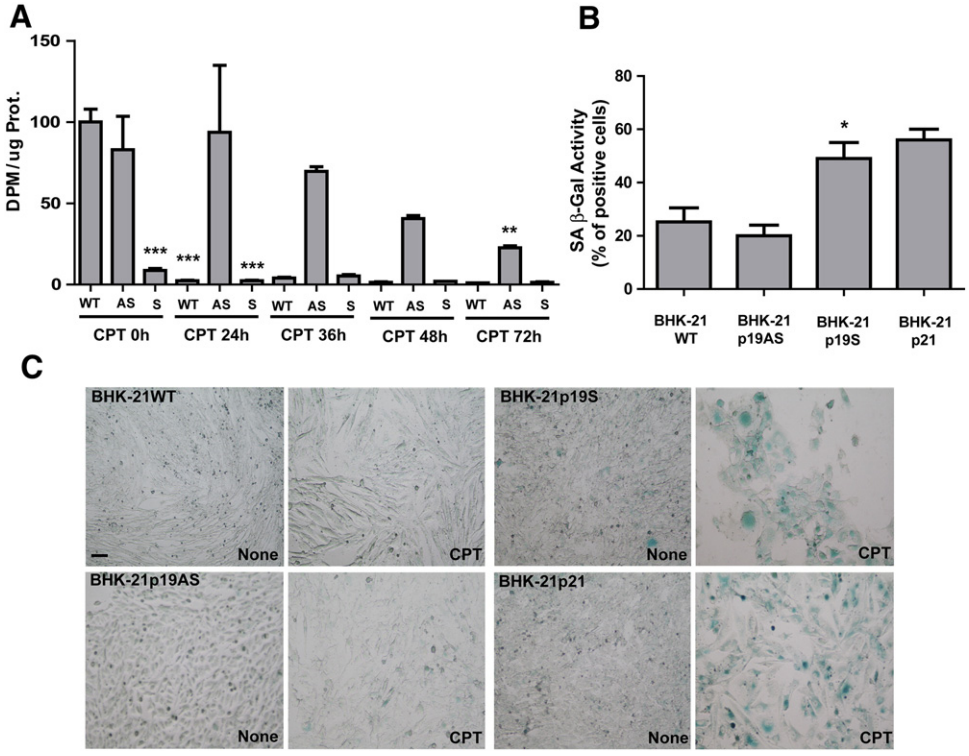

Fig. 2. Senescence-associated biomarkers are modulated by p19 levels. (A–C) BHK-21p19WT, BHK-21p19AS and BHK-21p19S cells were incubated with 75 μM $ZnSO_4$ for 5 h before being treated with 20 nM CPT. (A) After CPT treatments for 24, 48 or 72 h cells were incubated with 1 μCi/ml [^{3}H]-thymidine for 6 h at 37 °C. Cells were lysed and thymidine incorporation was measured as DPM/μg protein. Results were statistically analyzed by one-way ANOVA followed by Bonferroni's post-test. $F_{14,30} = 9.73$, ***$p < 0.0001$; WT 0 h vs. S 0 h, ***$p < 0.001$; WT 0 h vs. WT 24 h, ***$p < 0.001$; WT 0 h vs. S 24 h, ***$p < 0.001$; WT 0 h vs. AS 72 h, **$p < 0.01$. (B) After CPT treatment for 72 h BHK-21p19WT, BHK-21p19AS and BHK-21p19S cells were cytochemically analyzed for SA-β-Gal activity at pH 6.0. BHK21-p21 cell line stably transfected with p21 cDNA in a sense orientation was used as control for positive SA-β-Gal activity. (C) Percentages of SA-β-Gal positively stained cells in (B) were quantified and are presented as mean ± SEM of three different experiments. Student's *t*-test was used to compare the SA-β-Gal activity in BHK-21p19WT vs. BHK-21p19S treated with CPT (*$p = 0.0483$) (scale bar 20 μm).

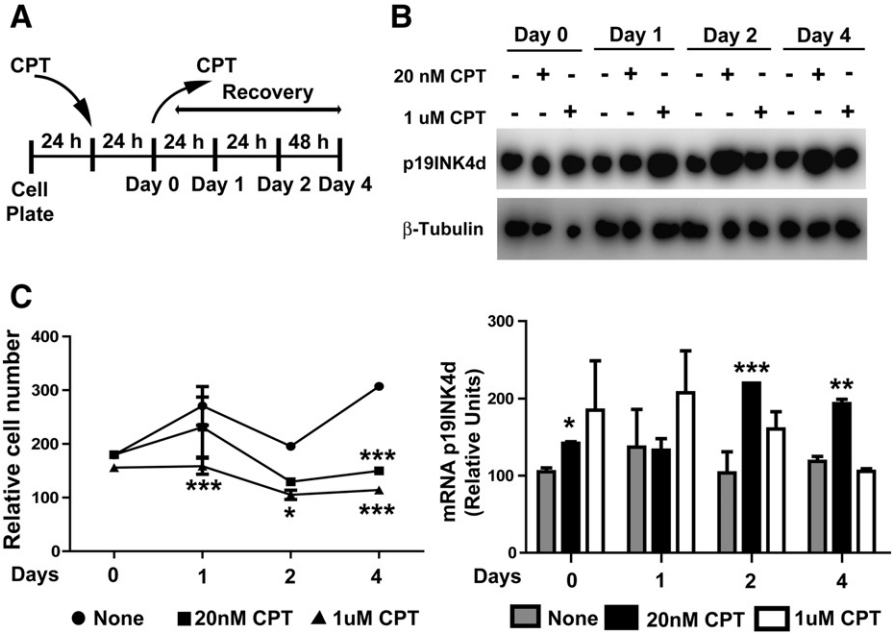

Fig. 3. Induction of p19 expression depends on genotoxic dose used. (A) Representative scheme that shows how the experiment was carried out and the time that each sample was taken. (B, C) WI-38 cells were pre-incubated with two different CPT concentrations (20 nM and 1 μM) for 24 h. Subsequently, the incubation was continued for 4 days in CPT-free medium. The samples were taken at the times indicated in A. (B) Total RNA was extracted and subjected to Northern blot analysis (upper panel). Northern blot quantification is showed in the lower panel. Bars represent the percentage of p19 expression with respect to no treated sample at day 0 which was set to 100%. Student's *t* test was used to compare each sample with no-treated sample at day 0 (*$p = 0.0103$; **$p = 0.0035$; ***$p = 0.0009$). (C) Cell proliferation assay measured by crystal violet staining. Values were normalized to the sample taken 24 h post plate which was set to 100%. The results were statistically analyzed by two-way ANOVA followed by Bonferroni's post-test. A significant main effect for treatment ($F_{2,15} = 22.27$, ***$p < 0.0001$), time ($F_{3,15} = 8.135$, ***$p = 0.0002$) and their interaction ($F_{6,15} = 4.307$, **$p < 0.0016$) was observed. Bonferroni's post-test reveals significant difference between, none vs. 20 nM CPT (day 4) ***$p < 0.001$; none vs. 1 μM CPT (day 1) ***$p < 0.001$, none vs. 1 μM CPT (day 2) *$p < 0.05$; none vs. 1 μM CPT (day 4) ***$p < 0.001$.

than at P3 (Fig. 4A). As a control, we checked the transcription of p21 and cyclin E. As expected, p21 showed a 2-fold increase while cyclin E showed a decrease in the transcription initiation rate for both senescence types.

To confirm these results, we carried out a gene reporter assay with a CAT reporter construct containing a 2250-bp fragment from the p19 promoter (p19CAT), which was transiently transfected in HEK293 cells treated or not with CPT and in MEFs at different passages. After 24 h of CPT treatment, we observed a remarkable induction of p19 promoter activity that was maintained for over 72 h (Fig. 4B). Likewise, a passage-dependent induction of p19 promoter activity became significant at P4-MEFs and remained elevated at P7-MEFs (Fig. 4C). Taken together, these results suggest that the senescence program up-regulates p19 expression by acting either directly or indirectly on its promoter.

We next examined the effect of both senescence types acting simultaneously on p19 promoter. To do this, MEFs at different passages were transiently transfected with p19CAT and treated with CPT to induce genotoxic senescence. We observed an additive effect on p19 transcriptional activity in CPT-treated MEFs at the last passage (Fig. 4D). This result suggests that both senescence types induce p19 through different cell signaling pathways.

3.5. Characterization of elements present in the p19 promoter involved in the senescence response

We have previously reported that the p19 promoter contains two functional E2F1 binding sites that appear to be sufficient to account for p19 up-regulation in both its cell cycle periodic expression pattern and in response to DNA damage [44]. To address whether these sites are involved in senescence-associated p19 induction, HEK293 cells were transiently transfected either with p19CAT or with a derived reporter plasmid in which both E2F binding sites were mutated (p19CATE2Fmut) (Supplementary Fig. S4A). We observed a CPT-mediated 3-fold increase in p19 promoter activity, which was nearly

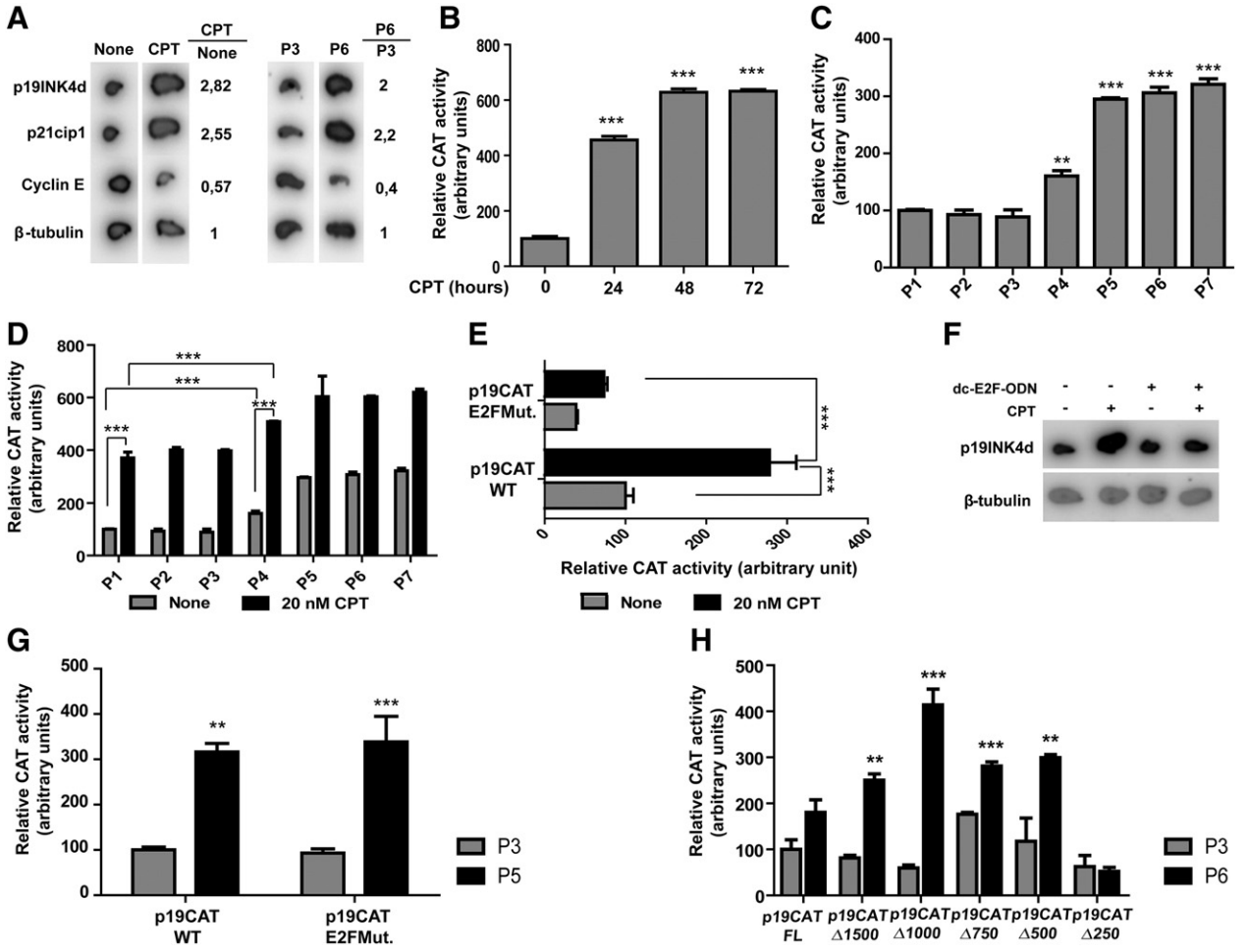

Fig. 4. p19 activation is regulated at transcriptional level during senescence. (A) WI-38 cells, treated or not with 20 nM CPT for 24 h, and MEFs, collected at P3 and P6, were subjected to nuclear run-on assay. Transcription rate of indicated genes was normalized to β-tubulin signal. Mean value of the transcription initiation rate is indicated at the right. (B) HEK293 cells, treated with 20 nM CPT at different time points and (C) MEFs, collected at different passages, were co-transfected with p19CAT (4 μg) and CMV-β-galactosidase (4 μg). CAT activity was determined and normalized to β-galactosidase activity. (B) Results were statistically analyzed by one-way ANOVA ($F_{3,8} = 572.1$, ***$p < 0.0001$) followed by Bonferroni's post-test ***$p < 0.001$ and (C) one-way ANOVA ($F_{6,21} = 161.4$, ***$p < 0.0001$), followed by Bonferroni's post-test **$p < 0.01$; ***$p < 0.001$. (D) MEFs at each passage were co-transfected as in (C) and treated or not with 20 nM CPT for 24 h. Student's *t* test was used to compare P1-p19CAT vs. CPT + P1-p19CAT, ***$p < 0.0001$; P1-p19CAT vs. P4-p19CAT, ***$p = 0.0003$; P4-p19CAT vs. CPT + P4-p19CAT, ***$p < 0.0001$; CPT + P1-p19CAT vs. CPT + P4-p19CAT, ***$p < 0.0004$. (E) HEK293 cells, co-transfected with p19CAT or p19CATE2Fmut and β-galactosidase, were treated or not with 20 nM CPT for 24 h. Results were statistically analyzed by one-way ANOVA followed by Bonferroni's post-test $F_{3,8} = 38.07$, ***$p < 0.0001$; none p19CAT vs. CPT + p19CAT, ***$p < 0.001$; CPT + p19CAT vs. CPT + p19CATE2Fmut, ***$p < 0.001$. (F) HEK293 cells, transfected with dc-E2F-ODN (100 nM) were treated with 20 nM CPT for 24 h. Total RNA was extracted and subjected to Northern blot analysis. (G) MEFs, collected from P3 and P5, were cotransfected with p19CAT or p19CATE2Fmut and β-galactosidase. Results were statistically analyzed by one-way ANOVA followed by Bonferroni's post-test $F_{3,12} = 19.52$, ***$p < 0.0001$, P3-p19CAT vs. P5-p19CAT, **$p < 0.01$; P3-p19CATE2Fmut vs. P5-p19CATE2Fmut, ***$p < 0.001$. (H) MEFs collected at P3 and P6, were transfected with a series of p19CATFL deletion mutants. Results were statistically analyzed by one-way ANOVA followed by Bonferroni's post-test $F_{11,24} = 27.16$, ***$p < 0.0001$; P3-p19CATΔ1500 vs. P6-p19CATΔ1500, **$p < 0.01$; P3-p19CATΔ1000 vs. P6-p19CATΔ1000, ***$p < 0.001$; P3-p19CATΔ750 vs. P6-p19CATΔ750, ***$p < 0.001$; P3-p19CATΔ500 vs. P6-p19CATΔ500, **$p < 0.01$.

blocked when the p19CATE2Fmut reporter gene was transfected (Fig. 4E; Supplementary Fig. S4B). To confirm these results, dumbbell-shaped decoy oligodeoxynucleotide (dc-E2F ODN), which contains the E2F consensus sequence, was used to sequester E2F transcription factors away from its target gene promoters [48]. Transfection of HEK293 cells with dc-E2F ODN and treatment with CPT for 24 h prevented the CPT-mediated induction of p19 (Fig. 4F). These results suggested that E2F1 alone is necessary to induce transcriptional activity of p19 promoter in genotoxic senescence.

To test the role of E2F binding sites in premature senescence, MEFs at P3 and P6 were transfected with the mentioned reporter constructs. Interestingly, a 3-fold increase in CAT activity was observed with both the wild type and mutated versions of the p19 promoter (Fig. 4G). Moreover, when both senescence types were jointly induced, the additive effect observed in p19 promoter activity was only partially reduced in p19CATE2Fmut transfected cells (Supplementary Fig. S4C). These results reinforce our hypothesis that both senescence types induce p19 through different signaling pathways.

Next, we aimed to identify *cis*-acting response elements in the 5′-flanking region of the p19 promoter responsible for its transcriptional activation during premature senescence. To this end, a series of progressively longer deletion mutants of p19CAT were constructed and transiently transfected into MEFs and assayed for CAT activity in the absence and presence of CPT (Supplementary Fig. S4A). Progressive deletion of p19 promoter did not significantly impair the p19 up-regulation in MEFs at P6. However, deletion of the region encompassing between −500 and −250 bp almost completely abolished the increase in CAT activity observed with the full-length promoter, suggesting that this region contains essential elements for p19 induction by premature senescence (Fig. 4H). Consistent with previous results (Fig. 4E), p19 up-regulated promoter activity of genotoxic associated-senescence was reduced when the E2F binding sites were deleted (Supplementary Fig. S4D).

3.6. Cell signaling pathways involved in p19 induction during senescence

Activation of ATM and ATR kinases represents very early DDR events. To explore the role of these proteins in senescence-associated p19 induction, we performed Northern blot analysis in the presence of caffeine or KU-55933, a phosphatidylinositol 3-kinase-related kinase inhibitor and a specific ATM inhibitor, respectively. Both inhibitors prevented p19 induction in genotoxic senescence and premature senescence (Fig. 5A and B, Supplementary Fig. S5A–C). Next, we asked whether downstream kinases, Chk1 or Chk2, are involved in p19 up-regulation, since both of them amplify the signal initiated by ATM/ATR. To test this, SB218078 and a Chk2 inhibitor were used. Results showed that only Chk1 inhibition impaired p19 induction in both senescence types (Fig. 5C and D).

It has been suggested that inactivation of p38SAPK (stress-activated protein kinase) delays the onset of various forms of cellular senescence [49,50]. We observed that specific inhibition of p38 caused a decreased in p19 induction by both genotoxic senescence and premature senescence (Fig. 5E and F). We conclude that p19 activation during senescence is triggered through a signaling pathway that includes, at least, ATM-Chk1 and probably p38.

3.7. p19 translocates to the nucleus and binds to the chromatin fraction following CPT treatment

It has been previously reported that p19 translocates from the cytoplasm to the nucleus following genotoxic insult [27,51]. To explore the cellular localization of p19 during senescence, CPT-treated HEK293 cells were subjected to sub-cellular fractionation. We observed that p19, mostly cytoplasmic in untreated cells, translocated to the nucleus upon CPT treatment and bound to the chromatin fraction (Fig. 6A). Interestingly, incubating the cells with Hoechst 33258, a DNA minor groove-binding agent, had an impact in p19 distribution displacing it from the chromatin fraction (Supplementary Fig. S6D).

In order to confirm this result but also to analyze the quality of the interaction between p19 and chromatin, we performed immunofluorescence experiments. WI-38 cells were treated or not with CPT for 72 h and incubated in the absence or in the presence of a detergent-containing buffer, prior to fixation, to eliminate the nucleoplasmic and chromatin soluble proteins. We confirmed that p19 translocated to the nucleus upon CPT treatment (Supplementary Fig. S6A–C). Moreover, both γ-HP1 and p19 resisted the detergent extraction and were detected in the nucleus, indicating that both proteins are strongly attached to chromatin (Fig. 6B and C). Furthermore, p19 appeared to have a localization pattern similar to γ-HP1 during senescence. Thereafter, CPT-treated cells were subjected to chromatin fractionation. p19 was predominantly detected in the α-HP1-rich fraction, corresponding to heterochromatin (Fig. 6D). Conversely, p19 was barely detected in the RNA polymerase II-rich fraction, corresponding to euchromatin.

3.8. p19 over-expression increases the global heterochromatinization triggered by genotoxic senescence

The partial co-localization of p19 with γ-HP1 and their presence in the α-HP1-rich chromatin fraction (Fig. 6) suggested the possibility that p19 might be involved in senescence playing a role in global heterochromatin formation. To test this, we first analyzed the expression of γ-HP1, a known SAHF marker, in BHK-21WT and in BHK-21p19S cells in the presence or absence of CPT. Interestingly, a higher increase in γ-HP1 was observed in BHK-21p19S than in BHK-21WT cells (Fig. 7A and B). Subsequently, we examined a potential role of p19 in the global chromatin structural change during genotoxic senescence looking at the in vivo MNase accessibility. We observed that the chromatin fraction from BHK-21p19AS cells was more sensitive to MNase digestion than that from BHK-21WT cells. In contrast, we found less digestion of the DNA obtained from the chromatin fraction isolated from CPT-treated BHK-21p19S cells than that from BHK-21WT cells (Fig. 7D). The data showed a lesser degree of chromatin condensation when p19 is down-regulated.

We also examined the electrostatic interaction between histones and chromatin DNA by extraction of histones with buffers containing different concentrations of NaCl (0.25 to 1 M). The extraction of total histone H3 was much lower in BHK-21p19S than in BHK-21WT cells at concentrations of 0.75 and 1 M NaCl. In addition, the amount of H3 extracted was greater in BHK-21p19AS at 0.5 M NaCl than in BHK-21WT (Fig. 7C). Together, these results suggest that the chromatin of p19 over-expressing cells undergoes electrostatic compaction during senescence.

p19 blocks the progression of the cell cycle by binding to either CDK4 or CDK6 and inhibiting the action of cyclin D [52]. To address whether p19 interaction with CDK4 is necessary to exert the observed effects in chromatin compaction during senescence, we performed transfection experiments by using a CDK4 mutated version (CDK4R24C) in BHK-21 WT and BHK-21p19S cells and then performed histone extraction. This mutant has a point mutation (replacement of Arg 24 by Cys) in the first coding exon and renders a variant that has full kinase activity but does not bind to and is therefore not inhibited by INK4 proteins [53]. Knock-in cells carrying this CDK4R24C mutant display proliferative advantages in vitro although they still display significant senescence-like features and resistance to cellular transformation [53–55]. The rationale was that if p19 exerts its action on heterochromatin formation during senescence in a CDK4-dependent manner, the combined over-expression of p19 and the mutant CDK4R24C should drive a decrease in heterochromatin formation and thereby an increase in histone extraction. The results show that the overexpression of CDK4R24C in BHK-21p19S did not modify the extraction of histones as compared with cells that only overexpressed p19 (BHK-21p19S) (Supplementary

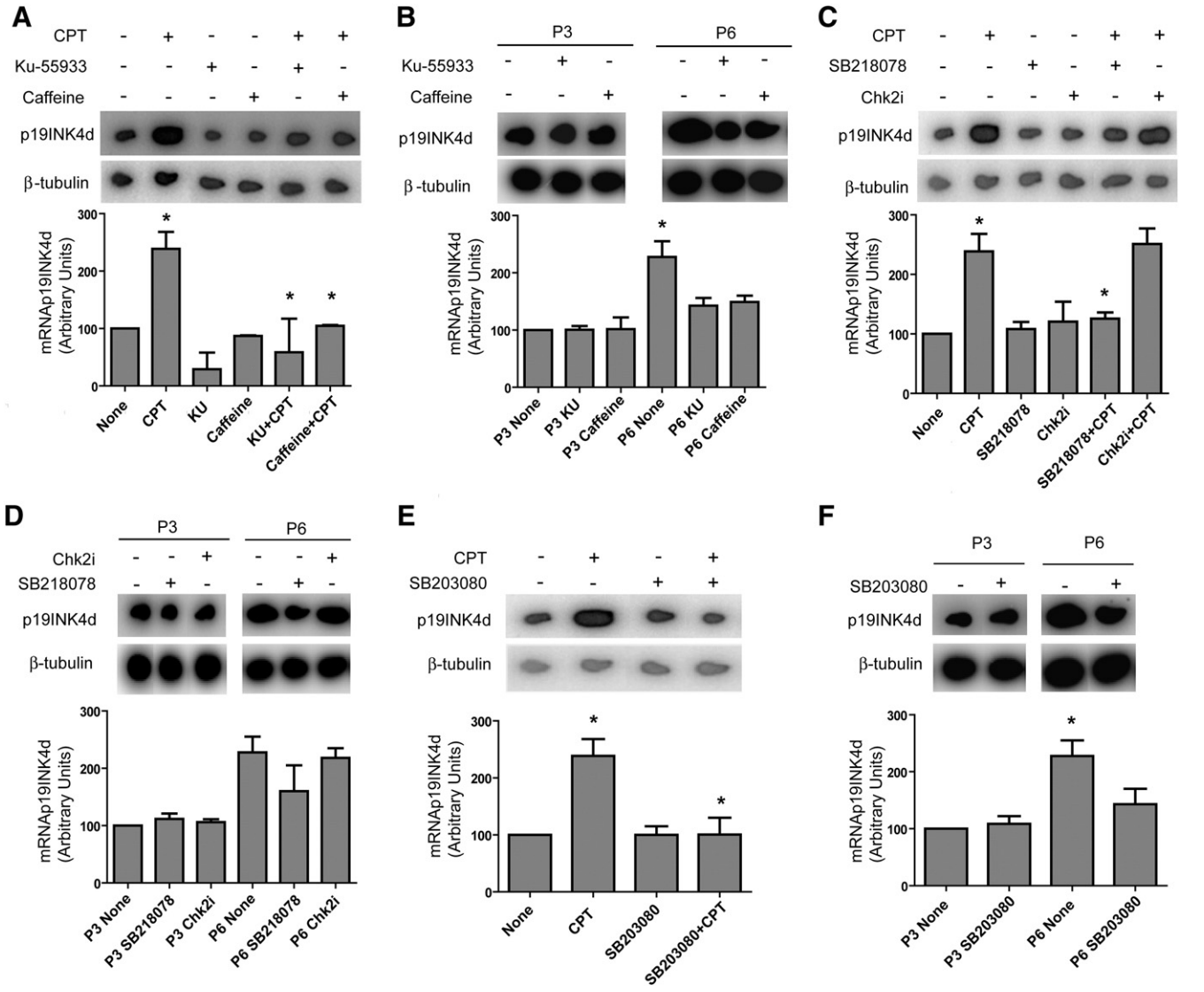

Fig. 5. Cell signaling pathways involved in p19 induction during senescence. WI-38 cells treated with 20 nM CPT and MEFs collected at P3 and P6 were incubated for 24 h with (A, B) 5 mM caffeine or 10 μM Ku-55933, (C, D) 15 nM SB218078 or 20 nM CHK2i or (E, F) 10 μM SB203080. Total RNA was extracted from cells and subjected to Northern blot analysis using a ^{32}P-labeled probe for p19 and β-tubulin. Northern blot quantifications are showed in the lower panels. Bars represent the percentage of p19 expression respect to non treated sample which was set to 100%. (A) Results were statistically analyzed by one-way ANOVA followed by Tukey's multiple comparison test $F_{5,6} = 25.97$, $^{***}p = 0.0005$; none vs. CPT, $^{*}p < 0.05$; CPT vs. Ku + CPT, $^{*}p < 0.05$; CPT vs. caffeine + CPT, $^{*}p < 0.05$. (B) $F_{5,6} = 9.71$, $^{**}p = 0.0077$; P3-none vs. P6-none, $^{**}p < 0.001$. (C) $F_{3,4} = 14.82$, $^{*}p = 0.0124$; none vs. CPT, $^{*}p < 0.05$; CPT vs. SB218078 + CPT, $^{*}p < 0.05$. (D) $F_{5,6} = 6.23$, $^{*}p = 0.0227$. (E) $F_{3,4} = 9.73$, $^{*}p = 0.0261$; none vs. CPT, $^{*}p < 0.05$; CPT vs. SB203080 + CPT, $^{*}p < 0.05$. (F) $F_{3,4} = 8.13$, $^{*}p = 0.0354$; P3-none vs. P6-none, $^{*}p < 0.05$.

Fig. S7A and B). These results strongly suggest that p19 exerts the mentioned effect in a CDK-4 independent manner.

3.9. In vivo age-dependent increase in p19 in different mouse tissues

We hypothesized that if p19 possesses a relevant effect associated with the establishment of senescence, its expression levels might be increased in tissues of aged organisms. Thus, we aimed to evaluate whether p19 induction during senescence is an event limited to cell lines and embryonic fibroblasts or, conversely, a phenotype associated with senescence. To confront this hypothesis, we analyzed p19 mRNA and protein expression in different mouse tissues at various ages. p19 mRNA levels increased proportionately with age in most tissues, except the thymus and pancreas (Fig. 8A and Supplementary Fig. S8A). We also examined p21 and p16 mRNA levels, and found that both senescence biomarkers were up-regulated in most tissues, in particular in those where p19 was not induced (thymus and pancreas). In contrast, in the brain and testicles, we observed high levels of p19 and p16 but not of p21.

Also, p19 protein levels significantly increased with age in most tissues except in the liver, pancreas and thymus (Fig. 8B and Supplementary Fig. S8B). When we graphed the data according to p19 expression at each age, we observed a tissue-independent increasing trend of p19 mRNA and protein expression with mouse age (Fig. 8C and D). These results indicate that p19 induction is not limited to cell cultures but also shows a positive correlation between p19 up-regulation and aging of mammals.

4. Discussion

Cellular senescence is an important mechanism of tumor suppression that prevents the proliferation of potential cancer cells [56,57]. Although most members of the CDK inhibitor (CKI) family are involved in the senescence response and the aging-dependent control of proliferation [55,58], in this work we showed for the first time that p19 is

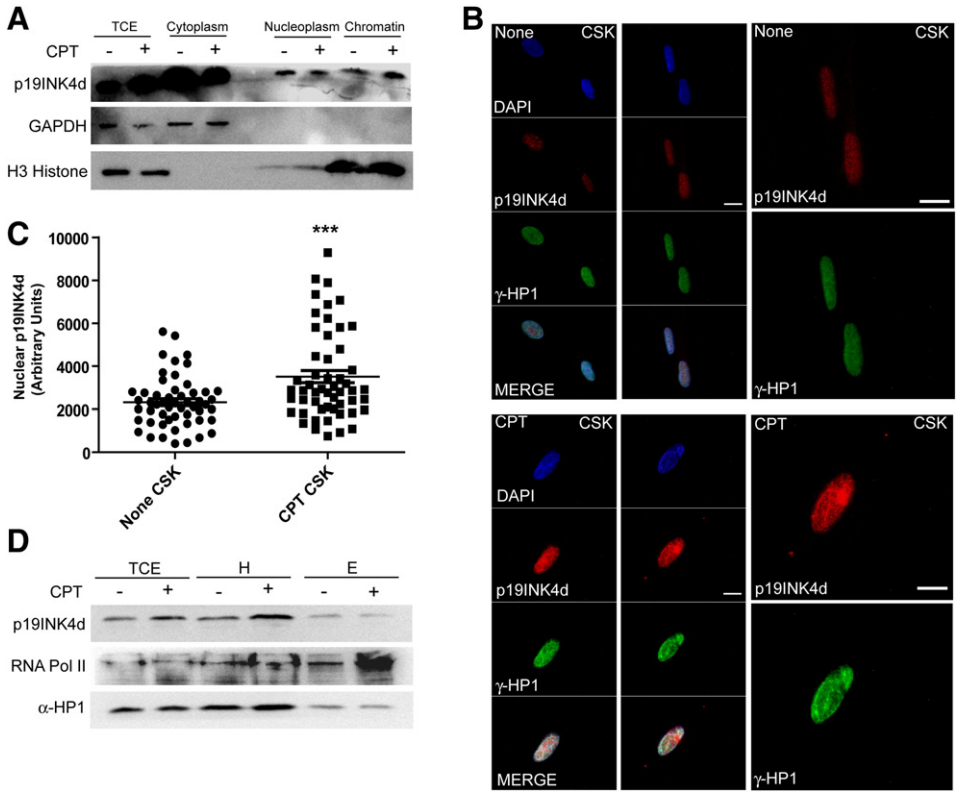

Fig. 6. p19 translocates to the nucleus and binds to the chromatin fraction following CPT treatment. (A) HEK293 cells were treated with 20 nM CPT for 24 h and were subjected to subcellular fractionation. The levels of indicated proteins were assessed by Western blot in the different fractions. GAPDH and H3 histone were used as markers of cytoplasm and chromatin fraction respectively. (B) Representative images of WI-38 cells treated or not with 20 nM CPT for 72 h. Prior to fixation cells were incubated with a detergent-containing buffer (cytoskeleton buffer, CSK) to discard soluble proteins. Localization of p19 (red) and γ-HP1 (green) was assessed through indirect immuno-fluorescence (scale bars 20 μm). Nuclear p19 was quantified and is presented in (C) as a mean ± SEM of 53 fields analyzed from three different experiments. Student's *t* test was used to compare none CSK vs. CPT CSK, $^{***}p = 0.0002$. (D) HEK293 cells were treated with 20 nM CPT for 24 h and subjected to nuclear fractionation. The levels of indicated proteins were assayed by Western blot; α-HP1 and RNAPolII were used as markers of heterochromatin and euchromatin fractions, respectively. Total cell extract (TCE), heterochromatin (H) and euchromatin (E).

induced not only in genotoxic senescence but also in premature senescence. Changes in two senescence-associated hallmarks, like cell cycle arrest and SA-β-gal activity, were affected by modulation of p19 expression. Furthermore, p19 up-regulation occurs simultaneously with the onset of senescence-associated cell markers. The beginning of p21 and p16 up-regulation temporarily coincides with p19 increase, thus indicating that p19 induction is an early event in the response to senescence stimuli.

Thereby, p19 would be a novel marker of senescence besides the canonical Rb/p16INK4a and p53/p21CIP1. In this regard, several reports postulate alternative pathways that, at least in some cell types and in some cellular contexts, may be the leading events driving to senescence. Concerning this subject, it has been demonstrated that in human mesenchymal stem cells the silencing of Rb1 triggers the activation of Rb2/p130, which leads to an irreversible cell cycle arrest and causes premature senescence [59]. p27Kip1 is another cell cycle inhibitor involved in cellular senescence. Up-regulation of p27Kip1 has been observed in aging tenocytes and has been associated with the process of replicative senescence [60]. Moreover, oridonin, a diterpenoid with a potent antitumoral activity, induces apoptosis and senescence in colorectal cancer cells by increasing the expression of p16INK4a, p21Cip1 and p27Kip1 [61]. Induction of the same cell cycle inhibitors has been reported to be associated with retinoic acid-mediated induction of cellular senescence in Huh7 and HCT116 cells [62].

The members of the CKI family are redundant in terms of their biological function which is associated with cell cycle arrest; however, they seem to be differentially regulated and apparently play distinct biological roles [23,63]. CKIs are commonly lost or inactivated by mutations in diverse types of cancer and represent established or candidate tumor suppressors [63]. p19 is not considered a tumor suppressor since p19 null mice do not develop proliferative disorders [64]. Nevertheless, some studies suggest the possibility that redundant functions "hide" the tumor suppressor activity of some family members. This is specially reflected in knock-out mice with more than one deleted CKI, which display higher tumor susceptibility than those with a single mutant [65–68]. A possible molecular basis for these biochemically indistinguishable molecules being able to carry out distinct tumor suppressive functions lies in the differences in their transcriptional regulation following diverse stimuli and the distinct and tissue-specific expression patterns [69,70]. A previous study has shown that histone deacetylase inhibitors induce the expression of p15 and p19 genes, causing growth arrest in p16INK4a-inactivated human cancer cells [71,72]. The induction of these genes by histone deacetylase inhibitors enables them to function as a replacement for p16INK4a in p16INK4a-inactivated cancer cells, since p15 and p19 are rarely mutated in human malignancies [52].

In addition, another recent study that analyzed 81 cases of various liver diseases including 51 cases of hepato-cellular carcinoma has shown that the frequent loss of p19 expression is associated not only with the development of this type of carcinoma but also with a poor prognosis of the disease [73]. Recent studies suggest that targeting specific CKIs in the appropriate genetic context can result in synthetic lethal interactions promoting a tumor-specific pro-senescence response with therapeutic benefits [74]. All this evidence suggests that p19 could be an under-covered tumor suppressor gene but that characteristic is not evident due to the redundant function of the CKI family.

We demonstrated that p19 induction is regulated at the transcriptional level and that the same signaling pathway seems to be involved in both genotoxic senescence and premature senescence. Nonetheless, this pathway does not converge in the activation of the

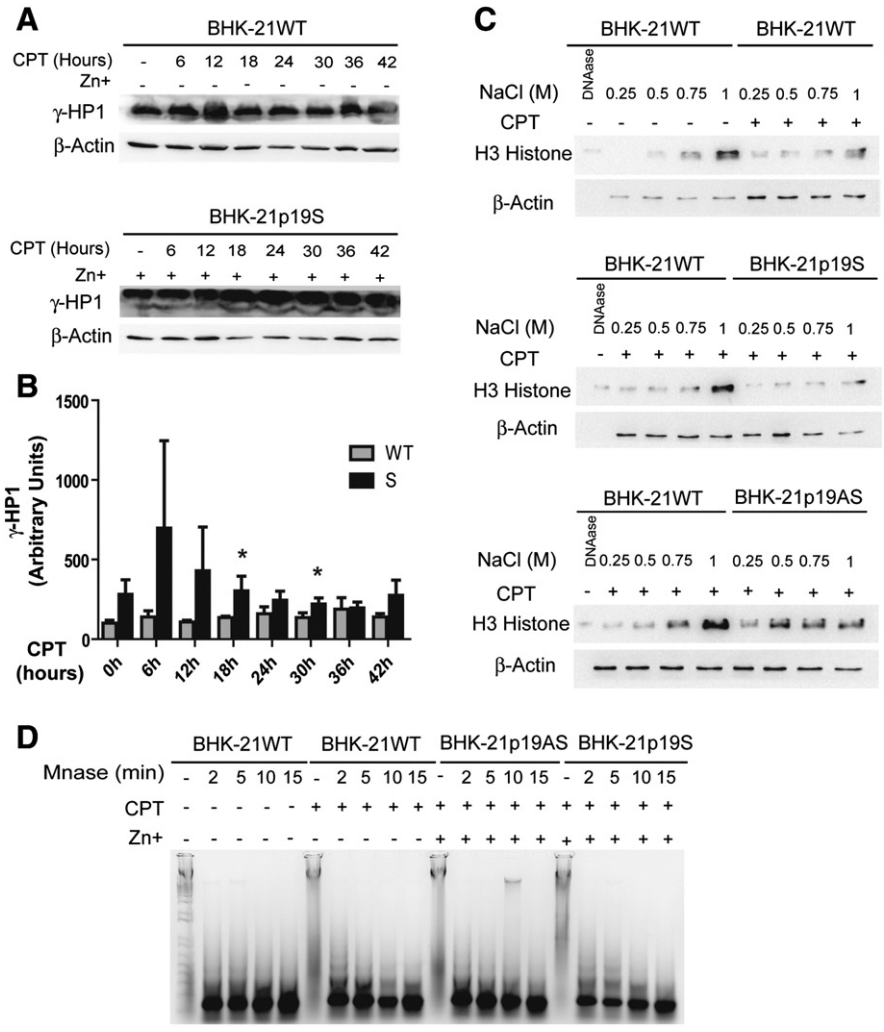

Fig. 7. p19 increases the global chromatin condensation. (A–D) BHK-21WT cells and BHK-21p19S or BHK21-p19AS were pre-incubated with 75 μM $ZnSO_4$ for 5 h. (A) BHK-WT and BHK-21p19S were incubated with 20 nM CPT for 42 h. Every 6 h samples were taken and equal amount of protein from cell lysates was subjected to 15% SDS-PAGE and analyzed by Western blot. γ-HP1 was quantified and is presented in (B) as a mean ± SEM of three different experiments. Student's *t* test was used to compare CPT-treated BHK-21WT vs CPT-treated BHK-21p19S (18 h, $^*p < 0.0370$); (30 h, $^*p < 0.0446$). (C) Nuclei from BHK-21WT (upper panel), BHK-21p19S (middle panel) and BHK-21p19AS (lower panel) cells treated with CPT for 72 h were isolated and assayed for histone core extraction with different NaCl concentrations. H3 histone was detected by Western blot. Results showed in the figure are representative of at least three independent experiments. (D) Nuclei from BHK-21WT, BHK-21p19S and BHK-21p19AS cells treated with CPT for 72 h were isolated and incubated with MNasa (0.2 U/μl) at different times after which, same amounts of DNA from each sample were subjected to agarose gel electrophoresis. Results showed in the figure are representative of at least three independent experiments.

same transcription factor. The E2F1 transcription factor is necessary to stimulate transcriptional activity of the p19 promoter when genotoxic senescence is induced. In contrast, p19 induction during premature senescence was independent of E2F1 but required the promoter region located between −500 and −250 bp. In silico analysis of this fragment revealed the presence of several Sp1 binding sites. This is particularly interesting because Sp1 is involved in senescence [75,76] and in p19 activation in response to histone deacetylase inhibitor treatment [72]. Furthermore, p38 plays a role in inducing senescence in response to various stimuli, especially stress due to reactive oxygen species [49,50]. Interestingly, p38 is also involved in Sp1 up-regulation during premature senescence [77]. This suggests that p38 could be involved in p19 induction through the activation of the Sp1 transcription factor in premature senescence.

Senescence is accompanied by extensive changes in chromatin structure. In particular, many senescent cells accumulate specialized domains of facultative heterochromatin, called SAHF [78,79]. In this work we showed that senescence stimuli caused p19 translocation to the nucleus where p19 binds to the chromatin enriched in HP1, suggesting its preferential interaction with heterochromatin. This interaction was resistant to detergent extraction indicating that p19 is tightly bound to chromatin. Our results prompted us to hypothesize that p19 induction cooperates with the formation of a higher-order chromatin structure based on inter-nucleosomal interaction associated with senescence. Several evidences support this hypothesis. p19 over-expressing senescent cells exhibit reduced MNase chromatin accessibility and increased γ-HP1 protein expression as compared to wild type and p19-deficient counterparts. In addition, susceptibility to histone extraction was diminished in p19 over-expressing cells. These results strongly suggest that, in response to senescence stimuli, p19 may be involved in global chromatin compaction. Precisely how p19 contributes to heterochromatin formation remains to be determined. However, our observation that cells pre-incubated with Hoechst, that bind to the minor groove of AT-rich DNA [80], displaced p19 from chromatin fractions, allows us to propose that p19 could bind to these sequences in senescent cells. This function of p19 is similar to that reported for HMGA protein [81], indicating that the central role of these proteins in senescence is to contribute to a repressive chromatin environment. In support of this hypothesis, previous experiments performed in our laboratory showed that p19 protein interacts with DNA with low sequence specificity. Another possibility is that p19 would interact with a chromatin remodeling factor altering its activity in such a way to promote

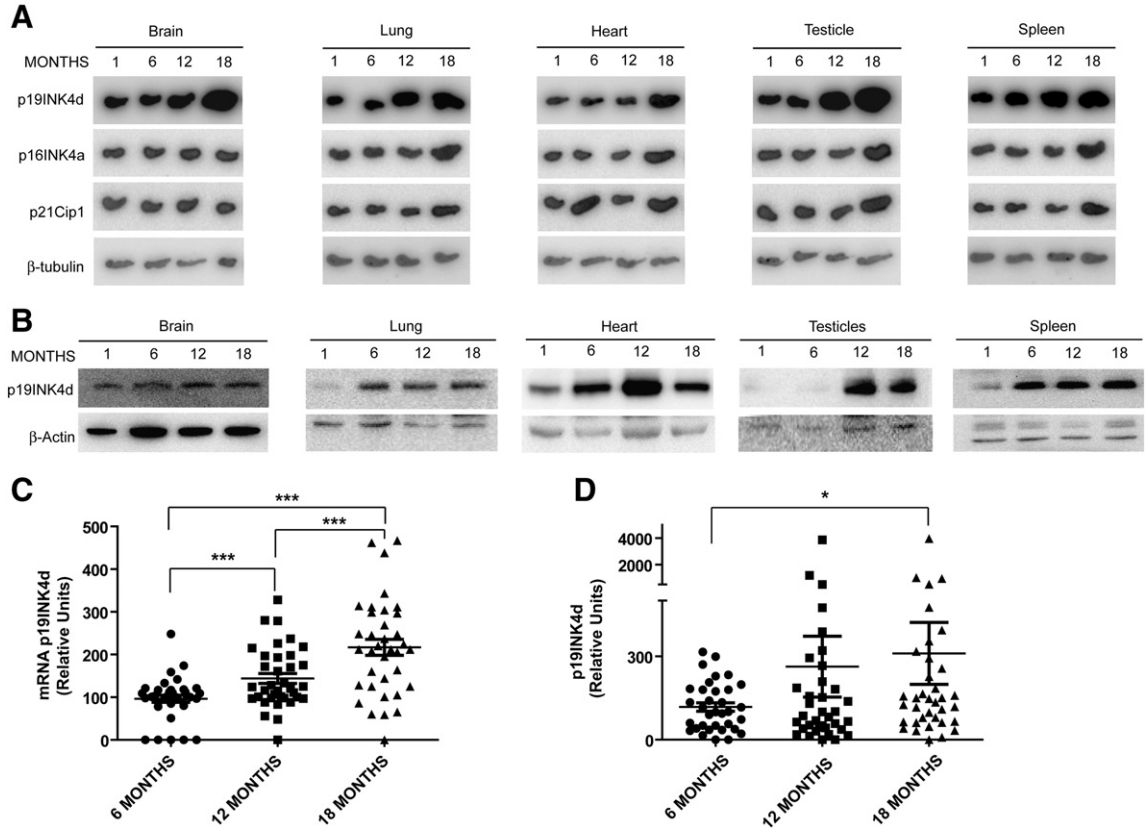

Fig. 8. Mice tissues display an age-dependent increase of p19 expression. (A, B) Samples extracted from several tissues of CF-1 male mice ($n = 4$) at different ages were subjected to (A) Northern blot assay with the ^{32}P-labeled probes indicated at the left margin and (B) Western blot assay with p19 and β-actin antibodies. (C) Quantification of p19 mRNA at each age was normalized to 1 month age sample. Student's *t* test was used to compare the levels of p19 expression (6 months vs. 12 months, $^{***}p < 0.0001$; 12 months vs. 18 months, $^{***}p = 0.0008$; 6 months vs. 18 months, $^{***}p = 0.0008$). (D) Quantification of p19 protein at each age was normalized to 1 month age sample. Student's *t* test was used to compare the levels of p19 protein expression (6 months vs. 18 months, $^{*}p < 0.05$).

heterochromatin formation. In this regard, Becker et al. have recently identified Brg1, a member of the SWI/SNF chromatin remodeling complex, as a novel binding partner of p16INK4a [82]. These authors propose that the p16INK4a–Brg1 complex regulates Brg1 chromatin remodeling activity. Moreover, it has been shown that Brg1 and its homologue, BRM, form an initiating component of heterochromatin complexes during the senescence of melanocytes [83,84]. Considering the structural similarity between INK4 family members, it is tempting to speculate that p19 could participate in a related mechanism. Interestingly, a yeast two-hybrid screen performed in our lab identified BRD7 as a potential p19-binding partner. As previously reported, BRD7 is required for the efficient induction of p-53 dependent oncogene-induced senescence [85].

Analysis of p19 mRNA and protein levels in several tissues from mice of different ages revealed an up-regulation of p19 that correlated with age. In most tissues, p19 induction temporarily matched with p16 and p21 up-regulation. However, several differences were observed, especially in the brain and testicles, tissues where p19 and p16 but not p21 were simultaneously up-regulated. On the other hand, the thymus and pancreas displayed a similar age-dependent increase in p16 and p21 expression and absence of p19 up-regulation. This different expression pattern and the concomitant expression of different members of the CKI family in distinct mouse tissues could be related to an overlapping function critical for tissue homeostasis [63]. Zindy et al. observed no age-associated p19 up-regulation [69]. These seemingly contradictory data are, at least in part, due to the differences in the experimental conditions used for protein extraction. Unlike us, this group discarded the nucleus from the total extract and in the present work we showed that p19 translocated to the nucleus in response to a senescent stimulus.

In summary, we propose that p19INK4d participates in the cellular mechanisms that trigger senescence by contributing to chromatin compaction. Furthermore, the present results indicate not only that p19 induction is not limited to the cell culture models used but also that there is a correlation between p19 expression and the aging of mammals. The elucidation of the mechanisms involved in senescence and the identification of the proteins that mediate its induction as well as its maintenance constitute important challenges for the development of therapeutic strategies aiming to overcome cancer and aging-associated disease.

Supplementary data to this article can be found online at http://dx.doi.org/10.1016/j.bbagen.2014.03.015.

Acknowledgements

This work was supported by research grants from the Agencia Nacional de Promoción Científica y Tecnológica (ANPCYT), Universidad de Buenos Aires (UBA) and Consejo Nacional de Investigaciones Científica y Técnicas (CONICET).

References

[1] I. Ben-Porath, R.A. Weinberg, The signals and pathways activating cellular senescence, Int. J. Biochem. Cell Biol. 37 (2005) 961–976.
[2] J. Campisi, F. d'Adda di Fagagna, Cellular senescence: when bad things happen to good cells, Nat. Rev. 8 (2007) 729–740.
[3] F. Rodier, J. Campisi, Cellular senescence: when bad things happen to good cells, Nat. Rev. 192 (2011) 547–556.
[4] T. Miura, M.P. Mattson, M.S. Rao, Cellular lifespan and senescence signaling in embryonic stem cells, Aging Cell 3 (2004) 333–343.

[5] F. d'Adda di Fagagna, Living on a break: cellular senescence as a DNA-damage response, Nat. Rev. Cancer 8 (2008) 512–522.
[6] F. d'Adda di Fagagna, S.H. Teo, S.P. Jackson, Functional links between telomeres and proteins of the DNA-damage response, Gene Dev. 18 (2004) 1781–1799.
[7] J.W. Shay, W.E. Wright, Senescence and immortalization: role of telomeres and telomerase, Carcinogenesis 26 (2005) 867–874.
[8] F. Rodier, J.P. Coppe, C.K. Patil, W.A. Hoeijmakers, D.P. Munoz, S.R. Raza, A. Freund, E. Campeau, A.R. Davalos, J. Campisi, Persistent DNA damage signalling triggers senescence-associated inflammatory cytokine secretion, Nat. Cell Biol. 11 (2009) 973–979.
[9] G. Sulli, R. Di Micco, F. d'Adda di Fagagna, Crosstalk between chromatin state and DNA damage response in cellular senescence and cancer, Nat. Rev. Cancer 12 (2006) 709–720.
[10] J. Gil, G. Peters, Regulation of the INK4b–ARF–INK4a tumour suppressor locus: all for one or one for all, Nat. Rev. 7 (2006) 667–677.
[11] S.L. Harris, A.J. Levine, The p53 pathway: positive and negative feedback loops, Oncogene 24 (2005) 2899–2908.
[12] F.A. Mallette, M.F. Gaumont-Leclerc, G. Ferbeyre, The DNA damage signaling pathway is a critical mediator of oncogene-induced senescence, Gene Dev. 21 (2007) 43–48.
[13] R. Funayama, F. Ishikawa, Cellular senescence and chromatin structure, Chromosoma 116 (2007) 431–440.
[14] R. Di Micco, M. Fumagalli, F. d'Adda di Fagagna, Breaking news: high-speed race ends in arrest—how oncogenes induce senescence, Trends Cell Biol. 17 (2007) 529–536.
[15] R. Zhang, W. Chen, P.D. Adams, Molecular dissection of formation of senescence-associated heterochromatin foci, Mol. Cell. Biol. 27 (2007) 2343–2358.
[16] M. Narita, S. Nunez, E. Heard, M. Narita, A.W. Lin, S.A. Hearn, D.L. Spector, G.J. Hannon, S.W. Lowe, Rb-mediated heterochromatin formation and silencing of E2F target genes during cellular senescence, Cell 113 (2003) 703–716.
[17] P. Oberdoerffer, S. Michan, M. McVay, R. Mostoslavsky, J. Vann, S.K. Park, A. Hartlerode, J. Stegmuller, A. Hafner, P. Loerch, S.M. Wright, K.D. Mills, A. Bonni, B.A. Yankner, R. Scully, T.A. Prolla, F.W. Alt, D.A. Sinclair, SIRT1 redistribution on chromatin promotes genomic stability but alters gene expression during aging, Cell 135 (2008) 907–918.
[18] R. Funayama, M. Saito, H. Tanobe, F. Ishikawa, Loss of linker histone H1 in cellular senescence, J. Cell Biol. 175 (2006) 869–880.
[19] Y. Kishi, Y. Fujii, Y. Hirabayashi, Y. Gotoh, HMGA regulates the global chromatin state and neurogenic potential in neocortical precursor cells, Nat. Neurosci 15 (2006) 1127–1133.
[20] R. Di Micco, G. Sulli, M. Dobreva, M. Liontos, O.A. Botrugno, G. Gargiulo, R. dal Zuffo, V. Matti, G. d'Ario, E. Montani, C. Mercurio, W.C. Hahn, V. Gorgoulis, S. Minucci, F. d'Adda di Fagagna, HMGA regulates the global chromatin state and neurogenic potential in neocortical precursor cells, Nat. Neurosci 13 (2006) 292–302.
[21] H.M. Chan, M. Narita, S.W. Lowe, D.M. Livingston, The p400 E1A-associated protein is a novel component of the p53 → p21 senescence pathway, Gene Dev. 19 (2005) 196–201.
[22] M. Narita, M. Narita, V. Krizhanovsky, S. Nunez, A. Chicas, S.A. Hearn, M.P. Myers, S. W. Lowe, A novel role for high-mobility group a proteins in cellular senescence and heterochromatin formation, Cell 126 (2006) 503–514.
[23] E.T. Canepa, M.E. Scassa, J.M. Ceruti, M.C. Marazita, A.L. Carcagno, P.F. Sirkin, M.F. Ogara, INK4 proteins, a family of mammalian CDK inhibitors with novel biological functions, IUBMB Life 59 (2007) 419–426.
[24] H. Hirai, M.F. Roussel, J.Y. Kato, R.A. Ashmun, C.J. Sherr, Novel INK4 proteins, p19 and p18, are specific inhibitors of the cyclin D-dependent kinases CDK4 and CDK6, Mol. Cell. Biol. 15 (1995) 2672–2681.
[25] T. Komata, T. Kanzawa, H. Takeuchi, I.M. Germano, M. Schreiber, Y. Kondo, S. Kondo, Antitumour effect of cyclin-dependent kinase inhibitors (p16(INK4A), p18(INK4C), p19(INK4D), p21(WAF1/CIP1) and p27(KIP1)) on malignant glioma cells, Br. J. Cancer 88 (2003) 1277–1280.
[26] N.E. Sharpless, M.R. Ramsey, P. Balasubramanian, D.H. Castrillon, R.A. DePinho, The differential impact of p16(INK4a) or p19(ARF) deficiency on cell growth and tumorigenesis, Oncogene 23 (2004) 379–385.
[27] J.M. Ceruti, M.E. Scassa, J.M. Flo, C.L. Varone, E.T. Canepa, Induction of p19INK4d in response to ultraviolet light improves DNA repair and confers resistance to apoptosis in neuroblastoma cells, Oncogene 24 (2005) 4065–4080.
[28] M.E. Scassa, M.C. Marazita, J.M. Ceruti, A.L. Carcagno, P.F. Sirkin, M. Gonzalez-Cid, O. P. Pignataro, E.T. Canepa, Cell cycle inhibitor, p19INK4d, promotes cell survival and decreases chromosomal aberrations after genotoxic insult due to enhanced DNA repair, DNA Repair (Amst) 6 (2007) 626–638.
[29] L. Tavera-Mendoza, T.T. Wang, B. Lallemant, R. Zhang, Y. Nagai, V. Bourdeau, M. Ramirez-Calderon, J. Desbarats, S. Mader, J.H. White, Convergence of vitamin D and retinoic acid signalling at a common hormone response element, EMBO Rep. 7 (2006) 180–185.
[30] F. Rodier, J. Campisi, Four faces of cellular senescence, J. Cell Biol. 192 (2011) 547–556.
[31] Y. Pommier, Topoisomerase I inhibitors: camptothecins and beyond, Nat. Rev. Cancer 6 (2006) 789–802.
[32] H.L. Cheng, S.M. Chang, Y.W. Cheng, H.J. Liu, Y.C. Chen, Characterization of the activities of p21Cip1/Waf1 promoter-driven reporter systems during camptothecin-induced senescence-like state of BHK-21 cells, Mol. Cell. Biochem. 291 (2006) 29–38.
[33] Z. Han, W. Wei, S. Dunaway, J.W. Darnowski, P. Calabresi, J. Sedivy, E.A. Hendrickson, K.V. Balan, P. Pantazis, J.H. Wyche, Role of p21 in apoptosis and senescence of human colon cancer cells treated with camptothecin, J. Biol. Chem. 277 (2002) 17154–17160.
[34] S. Parrinello, E. Samper, A. Krtolica, J. Goldstein, S. Melov, J. Campisi, Oxygen sensitivity severely limits the replicative lifespan of murine fibroblasts, Nat. Cell Biol. 5 (2003) 741–747.
[35] T. Kuilman, C. Michaloglou, W.J. Mooi, D.S. Peeper, The essence of senescence, Genes Dev. 24 (2010) 2463–2479.
[36] D.A. Conner, Mouse embryo fibroblast (MEF) feeder cell preparation, Curr. Protoc. Mol. Biol. (2001) 22 (Chapter 23:Unit 23).
[37] J.M. Ceruti, M.E. Scassa, M.C. Marazita, A.C. Carcagno, P.F. Sirkin, E.T. Canepa, Transcriptional upregulation of p19INK4d upon diverse genotoxic stress is critical for optimal DNA damage response, Int. J. Biochem. Cell Biol. 41 (2009) 1344–1353.
[38] C.L. Varone, E.T. Canepa, Evidence that protein kinase C is involved in delta-aminolevulinate synthase expression in rat hepatocytes, Arch. Biochem. Biophys. 341 (1997) 259–266.
[39] J. Mendez, B. Stillman, Chromatin association of human origin recognition complex, cdc6, and minichromosome maintenance proteins during the cell cycle: assembly of prereplication complexes in late mitosis, Mol. Cell. Biol. 20 (2000) 8602–8612.
[40] J.H. Frenster, V.G. Allfrey, A.E. Mirsky, Repressed and active chromatin isolated from interphase lymphocytes, Proc. Natl. Acad. Sci. U. S. A. 50 (1963) 1026–1032.
[41] E. Meshorer, D. Yellajoshula, E. George, P.J. Scambler, D.T. Brown, T. Misteli, Hyperdynamic plasticity of chromatin proteins in pluripotent embryonic stem cells, Dev. Cell 10 (2006) 105–116.
[42] B. Levy-Wilson, C. Fortier, B.D. Blackhart, B.J. McCarthy, DNase I- and micrococcal nuclease-hypersensitive sites in the human apolipoprotein B gene are tissue specific, Mol. Cell. Biol. 8 (1988) 71–80.
[43] R. Amouroux, A. Campalans, B. Epe, J.P. Radicella, Oxidative stress triggers the preferential assembly of base excision repair complexes on open chromatin regions, Nucleic Acids Res. 38 (2010) 2878–2890.
[44] A.L. Carcagno, M.C. Marazita, M.F. Ogara, J.M. Ceruti, S.V. Sonzogni, M.E. Scassa, L.E. Giono, E.T. Canepa, E2F1-mediated upregulation of p19INK4d determines its periodic expression during cell cycle and regulates cellular proliferation, PLoS One 6 (2011) e21938.
[45] Y. Durocher, S. Perret, A. Kamen, High-level and high-throughput recombinant protein production by transient transfection of suspension-growing human 293-EBNA1 cells, Nucleic Acids Res. 30 (2002) E9.
[46] C.L. Varone, L.E. Giono, A. Ochoa, M.M. Zakin, E.T. Canepa, Transcriptional regulation of 5-aminolevulinate synthase by phenobarbital and cAMP-dependent protein kinase, Arch. Biochem. Biophys. 372 (1999) 261–270.
[47] G.P. Dimri, X. Lee, G. Basile, M. Acosta, G. Scott, C. Roskelley, E.E. Medrano, M. Linskens, I. Rubelj, O. Pereira-Smith, et al., A biomarker that identifies senescent human cells in culture and in aging skin in vivo, Proc. Natl. Acad. Sci. U. S. A. 92 (1995) 9363–9367.
[48] K.K. Park, J. Deok Ahn, I.K. Lee, J. Magae, N.H. Heintz, J.Y. Kwak, Y.C. Lee, Y.S. Cho, H.C. Kim, Y.M. Chae, Y. Ho Kim, C.H. Kim, Y.C. Chang, Inhibitory effects of novel E2F decoy oligodeoxynucleotides on mesangial cell proliferation by coexpression of E2F/DP, Biochem. Biophys. Res. Commun. 308 (2003) 689–697.
[49] H. Iwasa, J. Han, F. Ishikawa, Mitogen-activated protein kinase p38 defines the common senescence-signalling pathway, Genes Cells 8 (2003) 131–144.
[50] F. Ishikawa, Cellular senescence, an unpopular yet trustworthy tumor suppressor mechanism, Cancer Sci. 94 (2003) 944–947.
[51] M.C. Marazita, M.F. Ogara, S.V. Sonzogni, M. Marti, N.J. Dusetti, O.P. Pignataro, E.T. Canepa, CDK2 and PKA mediated-sequential phosphorylation is critical for p19INK4d function in the DNA damage response, PLoS One 7 (2012) e35638.
[52] M.F. Roussel, The INK4 family of cell cycle inhibitors in cancer, Oncogene 18 (1999) 5311–5317.
[53] R. Sotillo, P. Dubus, J. Martin, E. de la Cueva, S. Ortega, M. Malumbres, M. Barbacid, Wide spectrum of tumors in knock-in mice carrying a Cdk4 protein insensitive to INK4 inhibitors, EMBO J. 20 (2001) 6637–6647.
[54] S.G. Rane, S.C. Cosenza, R.V. Mettus, E.P. Reddy, Germ line transmission of the Cdk4(R24C) mutation facilitates tumorigenesis and escape from cellular senescence, Mol. Cell. Biol. 22 (2002) 644–656.
[55] V. Quereda, J. Martinalbo, P. Dubus, A. Carnero, M. Malumbres, Genetic cooperation between p21Cip1 and INK4 inhibitors in cellular senescence and tumor suppression, Oncogene 26 (2007) 7665–7674.
[56] J. Campisi, Cellular senescence as a tumor-suppressor mechanism, Trends Cell Biol. 11 (2001) S27–S31.
[57] R. Sager, Senescence as a mode of tumor suppression, Environ. Health Perspect. 93 (1991) 59–62.
[58] V. Janzen, R. Forkert, H.E. Fleming, Y. Saito, M.T. Waring, D.M. Dombkowski, T. Cheng, R.A. DePinho, N.E. Sharpless, D.T. Scadden, Stem-cell ageing modified by the cyclin-dependent kinase inhibitor p16INK4a, Nature 443 (2006) 421–426.
[59] N. Alessio, W. Bohn, V. Rauchberger, F. Rizzolio, M. Cipollaro, M. Rosemann, M. Irmler, J. Beckers, A. Giordano, U. Galderisi, Silencing of RB1 but not of RB2/P130 induces cellular senescence and impairs the differentiation potential of human mesenchymal stem cells, Cell. Mol. Life Sci. 70 (2013) 1637–1651.
[60] W.C. Tsai, H.N. Chang, T.Y. Yu, C.H. Chien, L.F. Fu, F.C. Liang, J.H. Pang, Decreased proliferation of aging tenocytes is associated with down-regulation of cellular senescence-inhibited gene and up-regulation of p27, J. Orthop. Res. 29 (2011) 1598–1603.
[61] F.H. Gao, X.H. Hu, W. Li, H. Liu, Y.J. Zhang, Z.Y. Guo, M.H. Xu, S.T. Wang, B. Jiang, F. Liu, Y.Z. Zhao, Y. Fang, F.Y. Chen, Y.L. Wu, Oridonin induces apoptosis and senescence in colorectal cancer cells by increasing histone hyperacetylation and regulation of p16, p21, p27 and c-myc, BMC Cancer 10 (2010) 610.

[62] S.H. Park, J.S. Lim, K.L. Jang, All-trans retinoic acid induces cellular senescence via up-regulation of p16, p21, and p27, Cancer Lett. 310 (2011) 232–239.
[63] M. Thullberg, J. Bartkova, S. Khan, K. Hansen, L. Ronnstrand, J. Lukas, M. Strauss, J. Bartek, Distinct versus redundant properties among members of the INK4 family of cyclin-dependent kinase inhibitors, FEBS Lett. 470 (2000) 161–166.
[64] F. Zindy, J. van Deursen, G. Grosveld, C.J. Sherr, M.F. Roussel, INK4d-deficient mice are fertile despite testicular atrophy, Mol. Cell. Biol. 20 (2000) 372–378.
[65] R. Wiedemeyer, C. Brennan, T.P. Heffernan, Y. Xiao, J. Mahoney, A. Protopopov, H. Zheng, G. Bignell, F. Furnari, W.K. Cavenee, W.C. Hahn, K. Ichimura, V.P. Collins, G.C. Chu, M.R. Stratton, K.L. Ligon, P.A. Futreal, L. Chin, Feedback circuit among INK4 tumor suppressors constrains human glioblastoma development, Cancer Cell 13 (2008) 355–364.
[66] M.R. Ramsey, J. Krishnamurthy, X.H. Pei, C. Torrice, W. Lin, D.R. Carrasco, K.L. Ligon, Y. Xiong, N.E. Sharpless, Expression of p16Ink4a compensates for p18Ink4c loss in cyclin-dependent kinase 4/6-dependent tumors and tissues, Cancer Res. 67 (2007) 4732–4741.
[67] S. Gagrica, S. Brookes, E. Anderton, J. Rowe, G. Peters, Contrasting behavior of the p18INK4c and p16INK4a tumor suppressors in both replicative and oncogene-induced senescence, Cancer Res. 72 (2012) 165–175.
[68] P. Krimpenfort, A. Ijpenberg, J.Y. Song, M. van der Valk, M. Nawijn, J. Zevenhoven, A. Berns, p15Ink4b is a critical tumour suppressor in the absence of p16Ink4a, Nature 448 (2007) 943–946.
[69] F. Zindy, D.E. Quelle, M.F. Roussel, C.J. Sherr, Expression of the p16INK4a tumor suppressor versus other INK4 family members during mouse development and aging, Oncogene 15 (1997) 203–211.
[70] Y. Matsuzaki, T. Sakai, INK4 family — a promising target for 'gene-regulating chemoprevention' and 'molecular-targeting prevention' of cancer, Environ. Health Prev. Med. 10 (2005) 72–77.
[71] T. Hitomi, Y. Matsuzaki, T. Yokota, Y. Takaoka, T. Sakai, p15(INK4b) in HDAC inhibitor-induced growth arrest, FEBS Lett. 554 (2003) 347–350.
[72] T. Yokota, Y. Matsuzaki, K. Miyazawa, F. Zindy, M.F. Roussel, T. Sakai, Histone deacetylase inhibitors activate INK4d gene through Sp1 site in its promoter, Oncogene 23 (2004) 5340–5349.
[73] A. Morishita, J. Gong, A. Deguchi, J. Tani, H. Miyoshi, H. Yoshida, T. Himoto, H. Yoneyama, H. Mori, K. Kato, K. Kurokohchi, K. Deguchi, K. Izuishi, Y. Suzuki, Y. Kushida, R. Haba, H. Iwama, S. Watanabe, J. D'Armiento, T. Masaki, Frequent loss of p19INK4D expression in hepatocellular carcinoma: relationship to tumor differentiation and patient survival, Oncol. Rep. 26 (2011) 1363–1368.
[74] J.C. Acosta, J. Gil, Senescence: a new weapon for cancer therapy, Trends Cell Biol. 22 (2012) 211–219.
[75] H. Rayess, M.B. Wang, E.S. Srivatsan, Cellular senescence and tumor suppressor gene p16, Int. J. Cancer 130 (2012) 1715–1725.
[76] J. Wu, L. Xue, M. Weng, Y. Sun, Z. Zhang, W. Wang, T. Tong, Sp1 is essential for p16 expression in human diploid fibroblasts during senescence, PLoS One 2 (2007) e164.
[77] A. Dasari, J.N. Bartholomew, D. Volonte, F. Galbiati, Oxidative stress induces premature senescence by stimulating caveolin-1 gene transcription through p38 mitogen-activated protein kinase/Sp1-mediated activation of two GC-rich promoter elements, Cancer Res. 66 (2006) 10805–10814.
[78] M. Narita, S. Nunez, E. Heard, A.W. Lin, S.A. Hearn, D.L. Spector, G.J. Hannon, S.W. Lowe, Rb-mediated heterochromatin formation and silencing of E2F target genes during cellular senescence, Cell 113 (2003) 703–716.
[79] P.D. Adams, Remodeling of chromatin structure in senescent cells and its potential impact on tumor suppression and aging, Gene 397 (2007) 84–93.
[80] M.Z. Radic, M. Saghbini, T.S. Elton, R. Reeves, B.A. Hamkalo, Hoechst 33258, distamycin A, and high mobility group protein I (HMG-I) compete for binding to mouse satellite DNA, Chromosoma 101 (1992) 602–608.
[81] M. Narita, V. Krizhanovsky, S. Nunez, A. Chicas, S.A. Hearn, M.P. Myers, S.W. Lowe, A novel role for high-mobility group a proteins in cellular senescence and heterochromatin formation, Cell 126 (2006) 503–514.
[82] T.M. Becker, S. Haferkamp, M.K. Dijkstra, L.L. Scurr, M. Frausto, E. Diefenbach, R.A. Scolyer, D.N. Reisman, G.J. Mann, R.F. Kefford, H. Rizos, The chromatin remodelling factor BRG1 is a novel binding partner of the tumor suppressor p16INK4a, Mol. Cancer 8 (2009) 4.
[83] D. Bandyopadhyay, J.L. Curry, Q. Lin, H.W. Richards, D. Chen, P.J. Hornsby, N.A. Timchenko, E.E. Medrano, Dynamic assembly of chromatin complexes during cellular senescence: implications for the growth arrest of human melanocytic nevi, Aging Cell 6 (2007) 577–591.
[84] N. Wajapeyee, R.W. Serra, X. Zhu, M. Mahalingam, M.R. Green, Oncogenic BRAF induces senescence and apoptosis through pathways mediated by the secreted protein IGFBP7, Cell 132 (2008) 363–374.
[85] J. Drost, F. Mantovani, F. Tocco, R. Elkon, A. Comel, H. Holstege, R. Kerkhoven, J. Jonkers, P.M. Voorhoeve, R. Agami, G. Del Sal, BRD7 is a candidate tumour suppressor gene required for p53 function, Nat. Cell Biol. 12 (2010) 380–389